MOLECULAR BIOLOGY

10.1126/sciadv.1501482

Highly sensitive sequencing reveals dynamic modifications and activities of small RNAs in mouse oocytes and early embryos

Qiyuan Yang,[1,2]* Jimin Lin,[1,2]* Miao Liu,[3]* Ronghong Li,[1,2] Bin Tian,[4] Xue Zhang,[1,2] Beiying Xu,[1,2] Mofang Liu,[2] Xuan Zhang,[3] Yiping Li,[2] Huijuan Shi,[3,5]† Ligang Wu[1,2]†

Small RNAs play important roles in early embryonic development. However, their expression dynamics and modifications are poorly understood because of the scarcity of RNA that is obtainable for sequencing analysis. Using an improved deep sequencing method that requires as little as 10 ng of total RNA or 50 oocytes, we profile small RNAs in mouse oocytes and early embryos. We find that microRNA (miRNA) expression starts soon after fertilization, and the mature miRNAs carried into the zygote by sperm during fertilization are relatively rare compared to the oocyte miRNAs. Intriguingly, the zygotic miRNAs display a marked increase in 3′ mono- and oligoadenylation in one- to two-cell embryos, which may protect the miRNAs from the massive degradation taking place during that time. Moreover, bioinformatics analyses show that the function of miRNA is suppressed from the oocyte to the two-cell stage and appears to be reactivated after the two-cell stage to regulate genes important in embryonic development. Our study thus provides a highly sensitive profiling method and valuable data sets for further examination of small RNAs in early embryos.

INTRODUCTION

In mammalian cells, small RNAs <35 nucleotides (nt) include three major classes: microRNA (miRNA), endogenous small interfering RNA (endo-siRNA), and Piwi-interacting RNA (piRNA). miRNAs are highly conserved ~21-nt-long small RNAs encoded by most eukaryotes (*1*). Long miRNA primary transcripts (pri-miRNAs) are cleaved by Drosha/DGCR8 into short hairpin structures of ~70 nt (pre-miRNAs) in the nucleus, followed by nuclear export through Exportin5 and further processing into mature miRNAs by the RNase III enzyme Dicer (*2*–*4*). Endo-siRNAs are structurally similar to miRNAs but are less conserved. They are usually processed from endogenous long RNA duplexes by Dicer (*1*, *5*). Both miRNAs and endo-siRNAs associate with Argonaute (AGO) proteins and participate in posttranscriptional gene regulation. miRNAs generally function through accelerating deadenylation and/or inhibiting the translation of target mRNAs by binding to partially complementary miRNA-responsive elements in the 3′ untranslated region (*6*), whereas endo-siRNAs exert their repressive effects by inducing endonucleolytic cleavage at perfectly complementary target sequences in mRNAs (*2*, *7*). piRNAs are single-stranded, 25- to 33-nt-long small RNAs that are associated with Piwi subfamily proteins (*8*–*10*). They are capable of repressing transposable elements, both transcriptionally and posttranscriptionally, and are indispensable for male fertility (*11*–*14*). In addition to distinct molecular features, the tissue distribution of these three classes of small RNAs is also different. miRNAs are widely expressed in diverse tissues, whereas endo-siRNAs and piRNAs are abundant in mammalian gametes (*10*, *15*, *16*).

Accumulating evidence has shown that small RNAs play important roles in oogenesis and early embryonic development (*17*, *18*). A previous profiling study showed a transition from a predominant presence of endo-siRNAs and piRNAs in oocytes to a miRNA majority in embryos during preimplantation development (*17*). The depletion of Dicer or AGO2 in oocytes leads to severe chromatin segregation defects during meiosis (*19*–*22*). The loss of AGO2 slicer activity results in a similar phenotype and is accompanied by increased retrotransposon activities, whereas oocytes develop normally in the absence of DGCR8; hence, endo-siRNAs, not miRNAs, are essential for oogenesis (*19*–*22*). In contrast, the zygotic knockout of DGCR8 or Dicer causes embryonic arrest at embryonic day (E) 6.5 or 7.5, indicating important functions of miRNAs in early embryonic development (*20*, *23*).

Maternal-to-zygotic transition (MZT) is the period when the transcription landscape in the early embryo undergoes a large-scale reprogramming, with maternally inherited RNAs being rapidly degraded and zygotic genes being extensively activated, resulting in a rapid cell fate transition from gametic to totipotent (*24*, *25*). The miR-430 family of the zebrafish, one of the most abundantly expressed miRNA families in early embryonic development, induces the deadenylation and degradation of many maternal mRNAs during MZT (*26*). A similar phenomenon was observed in *Xenopus laevis* through the action of the miR-427 family (*27*). The miR-294 family, a homolog of zebrafish miR-430, has been cloned in mice (*28*), whose deficiency causes partially penetrant embryonic lethality at mid-late gestation (*29*), raising the possibility that this mechanism may be conserved in all vertebrates. However, more recent studies have shown that miRNA functions are suppressed in mouse oocytes (*22*, *30*), casting doubt on the role of mammalian miRNAs in maternal mRNA degradation and raising the question as to when the activity of miRNAs is restored in early embryonic development.

Unlike microarrays or quantitative reverse transcription polymerase chain reaction (qRT-PCR), which can only detect known small RNAs,

[1]State Key Laboratory of Molecular Biology, National Center for Protein Science Shanghai, Shanghai Science Research Center, Shanghai Institute of Biochemistry and Cell Biology, Shanghai Institutes for Biological Sciences, University of Chinese Academy of Sciences, Chinese Academy of Sciences, Shanghai 200031, China. [2]Shanghai Key Laboratory of Molecular Andrology, Shanghai Institute of Biochemistry and Cell Biology, Shanghai Institutes for Biological Sciences, Chinese Academy of Sciences, Shanghai 200031, China. [3]China National Population and Family Planning Key Laboratory of Contraceptive Drugs and Devices, Shanghai Institute of Planned Parenthood Research, Shanghai 200032, China. [4]Department of Microbiology, Biochemistry and Molecular Genetics, Rutgers New Jersey Medical School, Newark, NJ 07103, USA. [5]Shanghai Key Laboratory of Reproductive Medicine, Shanghai Jiao Tong University, Shanghai 200025, China.
*These authors contributed equally to this work.
†Corresponding author. Email: shihuijuan2011@163.com (H.S.); lgwu@sibcb.ac.cn (L.W.)

deep sequencing has the ability to profile small RNAs with diverse sequences, including endo-siRNAs and piRNAs, and identify new small RNAs and their sequence variations. However, the construction of small RNA complementary DNA (cDNA) libraries for deep sequencing usually requires several hundred nanograms of total RNA, corresponding to thousands of oocytes or zygotes, which are not readily obtainable. As a consequence, few analyses have been conducted using deep sequencing to profile small RNAs in the early embryos of mammals (*15*–*17*, *31*), limiting the understanding of the expression dynamics and modifications of small RNAs, as well as their functions during early stages of embryonic development. Here, we improve the cDNA library construction method for analyzing small RNAs by deep sequencing, which reduces the input requirement to fewer than 50 oocytes, making it feasible to analyze small RNA expression without large-scale preparation of embryos. Using this method, we profile small RNAs in mouse oocytes and embryos from one- (1C) to eight-cell (8C) stages. We observe extensive mono- and oligo-A tailing on many miRNAs at 1C and two-cell (2C) stages, which may function to stabilize them during the large-scale miRNA degradation in MZT. Furthermore, our bioinformatics analyses indicate that the function of miRNAs is suppressed from the oocyte to 1C stages but is reactivated after the 2C stage. Additionally, we provide evidence that sperm-borne miRNAs carried into the zygote by fertilization are extremely rare. Our results are valuable for deciphering the turnover mechanisms and functions of small RNAs in early embryos of mammals.

RESULTS AND DISCUSSION

Improving the sensitivity for profiling small RNAs by deep sequencing

Profiling of small RNAs by deep sequencing usually requires hundreds of nanograms of total RNA (*16*, *17*, *32*). A low input of RNA results in predominant ligation products being those between the 5′ and 3′ adapters, severely compromising subsequent PCR amplification and usability of sequencing reads. We improved the method for cDNA library construction of small RNAs for deep sequencing by optimizing the conditions for the 5′ and 3′ adapter ligation and PCR amplification steps (Fig. 1A and Materials and Methods), effectively reducing the minimal requirement of input RNA. In the tested range (1 to 100 ng) of total RNA from human embryonic kidney (HEK) 293 cells, technical replicates of 100, 33, and 10 ng of total RNAs showed excellent correlations (Spearman correlation coefficient $R > 0.94$, Pearson correlation coefficient $R > 0.99$) in miRNA profiles (Fig. 1B and fig. S1A) and could reliably examine both highly and lowly abundant miRNAs with expression difference >10,000-fold (Fig. 1, C and D). In contrast, a lower (1- to

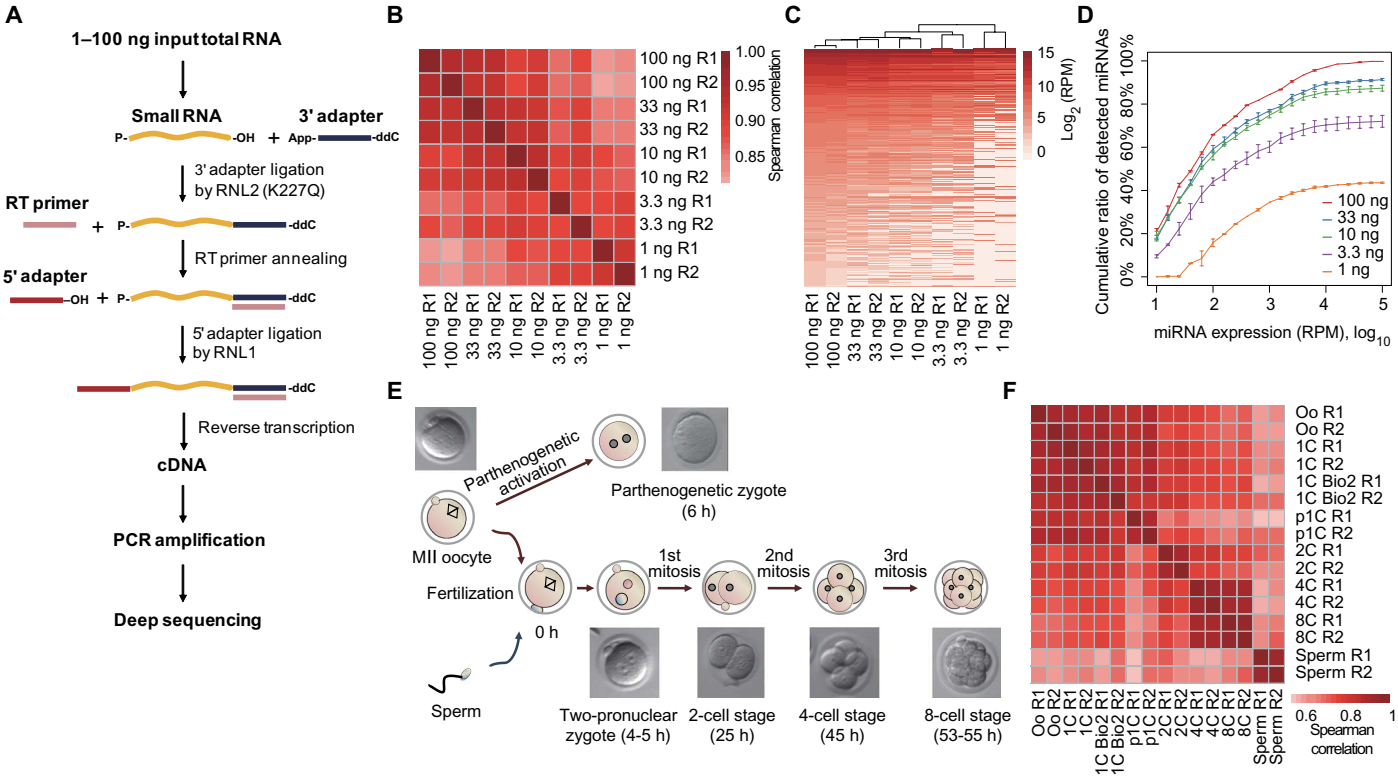

Fig. 1. Sensitivity and reproducibility of the improved method for profiling small RNAs by deep sequencing. (**A**) Diagram of the workflow for constructing the cDNA library of small RNAs for deep sequencing. (**B**) Spearman correlation heat map of the miRNA profiles generated from 1 to 100 ng of total RNA of HEK293 cells. (**C**) Unsupervised hierarchical clustering of miRNA profiles. Only miRNAs with reads per million (RPM) >1 in both of the 100-ng technical replicates are shown. (**D**) Cumulative ratio of miRNAs detected in 1 to 100 ng of total RNA, as described in (B). The miRNAs were ranked by using the average expression of two replicates. miRNAs with an RPM >1 in both of the 100-ng replicates are used for the analysis, and the SDs within each group are reported. (**E**) Collected mouse oocyte and embryo samples at different developmental stages for small RNA sequencing. (**F**) Spearman correlation heat map of the miRNA profiles of the early embryonic samples in (E). R1 and R2 represent technical replicates. Bio2 represents biological replicates.

3.3-ng) input of total RNA showed significantly reduced correlation coefficients between replicates and decreased sensitivity in detecting lowly abundant miRNAs, suggesting that input RNA of 10 ng was the lower bound of the method. To test the robustness of the method, we performed additional sequencing of small RNAs from different human cell lines, including HeLa, A549, and HEK293. All of the biological replicates that used an input of 10 ng of total RNA consistently showed excellent correlation in miRNA profiles and reasonable correlation with the results generated using 100 ng of total RNA (fig. S1B). It is notable that the variability of lowly abundant miRNAs was greater than that of highly abundant ones (fig. S1B), causing the difference between Pearson and Spearman correlation coefficients. We further analyzed the expression of miRNAs in these cell lines by qRT-PCR. The results showed that the relative abundance of miRNAs between any two cell lines quantified by qRT-PCR was comparable to that calculated from the deep sequencing results with 10 or 100 ng of input RNA (fig. S1, C and D), indicating that our improved method reliably measures the relative abundance of small RNAs. When the method was further applied to sequencing small RNAs in mouse oocytes and zygotes (1C) using 10 ng of total RNA (corresponding to <50 oocytes or zygotes), both biological and technical replicates of miRNA expression were highly reproducible (Fig. 1, E and F, and fig. S1E). These results indicate that the performance of the improved small RNA sequencing method was robust and can be applied to other studies where RNA material is scarce.

Dynamic expressions of small RNAs in oocytes and early embryos

Using our optimized library construction method, we profiled small RNAs in the oocytes (Oo), 1C (or zygote), parthenogenetic one-cell (p1C), 2C, four-cell (4C), and 8C embryos of mouse (Fig. 1, E and F). Each small RNA library was generated from <50 oocytes or embryos, and technical duplicates showed excellent correlations in miRNA profiling (Fig. 1F and data set S1). In contrast to the single peak of ~22-nt small RNAs in $CD4^+$ T cells, which served as a somatic cell control, the size distribution of the small RNAs in the oocytes and embryos showed a bimodal pattern (Fig. 2A). The peak centered at 22 nt was composed of miRNAs, endo-siRNAs, and short small RNAs derived from repetitive elements, and the second peak at 29 nt corresponded to piRNAs and small RNAs derived from repetitive elements and transfer RNA (tRNA) fragments, consistent with previous reports (*15*–*17*). The fraction of miRNAs increased rapidly by fourfold during early development, whereas piRNAs, endo-siRNAs, and other repetitive element–derived small RNAs decreased by more than twofold (Fig. 2B), also consistent with previous studies (*17*, *18*). More than 80% of endo-siRNAs and piRNAs were mapped to repetitive sequences, with particular enrichment for the LINE (long interspersed nuclear element) and LTR (long terminal repeat) families (Fig. 2, C and D, and data set S1), in agreement with their functions in repressing transposable elements during early embryonic development (*15*, *16*, *33*). It was reported that some tRNA-derived fragments can perform functions in cancer cells (*34*). Moreover, recent studies have shown that sperm can carry tRNA fragments and perform important functions in embryonic development (*35*, *36*). Intriguingly, we observed that several tRNA-derived small RNAs (≥30 nt), including those from glycine, glutamine, and valine tRNAs, significantly increased during development and became fairly abundant at the 8C stage (data set S1). These tRNA-derived small RNAs may have unknown biological functions that warrant further investigation.

The expression of miRNAs was dynamically regulated in early embryos (Fig. 3A). A total of 458 known miRNAs were detected in the Oo-8C stages, of which 183 were expressed with RPM ≥20 at least at one stage (Fig. 3A and data set S1). Notably, we found that besides the conserved miRNAs, such as the previously reported Let-7 and miR-30 families, several nonconserved miRNAs, including miR-871-3p, miR-741-3p, and miR-470-5p, were also among the 10 most abundant miRNAs in the oocytes in our sequencing data. These three nonconserved miRNAs are located within a 20-kb genomic region and are transcribed as a single transcript, which argues against the possibility that they are artifacts caused by spurious ligation products. Notably, these nonconserved miRNAs were absent from previous studies using microarrays or qRT-PCR because they were not included in the probe sets (*18*, *37*). It is well known that the first wave of zygotic gene activation (ZGA) is in the middle S phase of 1C, namely, minor ZGA (*38*, *39*), and that many more zygotic genes start to express at the 2C stage, known as major ZGA, followed by another wave of embryonic gene activation in 4C-8C, namely, mid-preimplantation gene activation (MGA). Our sequencing results showed that the miRNAs could also be clustered into several distinct groups, including maternal, maternal to ZGA, maternal to MGA, ZGA, MGA, and others, according to their expression patterns (Fig. 3B). By comparing the small RNA profiles between the oocytes and zygotes, we found that the first wave of miRNA production can be detected in the zygotes as early as about 5 hours after fertilization in vivo. During the 1C-to-2C transitions, 72 miRNAs were up-regulated. After the 2C stage, 112 miRNAs were markedly up-regulated, the number of which was much higher than that of down-regulated ones. Parallel to the large-scale clearance of maternal mRNAs in 1C to 4C, many maternal miRNAs were down-regulated greater than twofold in Oo-1C and 1C-2C (Fig. 3C). Intriguingly, the degradation of miRNAs was significantly slowed down in 2C-4C and 4C-8C, suggesting that the extensive degradation of maternal miRNAs occurred approximately at the 2C stage (Fig. 3C). These substantial changes reflect that replacing maternal miRNAs with zygotic miRNAs at the onset of major ZGA may contribute to gene regulation that is essential for embryonic development. The number of miRNAs undergoing degradation and their decay rate may not be accurate because the relative expression level of an individual miRNA would be influenced by changes in the abundance of other small RNAs in the same cell. Previous profiling with single-cell qRT-PCR arrays, a ligation-independent quantification method, has shown that the total amount of miRNA in the 2C embryo was significantly less than that in zygotes (*18*), suggesting that the abundance of miRNAs in the 2C embryo may be overestimated in our current analyses and that the decay rate of parental miRNAs is likely to be even faster. In future studies, spike-in RNAs with known quantities are needed for more accurate quantification of small RNAs.

Minuscule contribution of sperm-borne miRNAs to zygotic miRNAs

In addition to the paternal genomic DNA, sperm contains distinct small RNAs that may be carried into the zygote during fertilization and contribute to early embryonic development. Previous studies have shown that parental small RNAs in gametes could mediate transgenerational inheritance in *Caenorhabditis elegans* and mouse (*40*, *41*). In mouse, miR-34c-5p was reported to be sperm-borne and essential for the first division of zygotes in one study (*42*) but was found to be dispensable for early development in another study (*43*). To identify the small RNAs delivered by a sperm to an oocyte during fertilization, we sequenced early pronucleus–stage 1C and p1C samples that were collected approximately 5 hours after fertilization, a time point when zygotic transcription has not yet

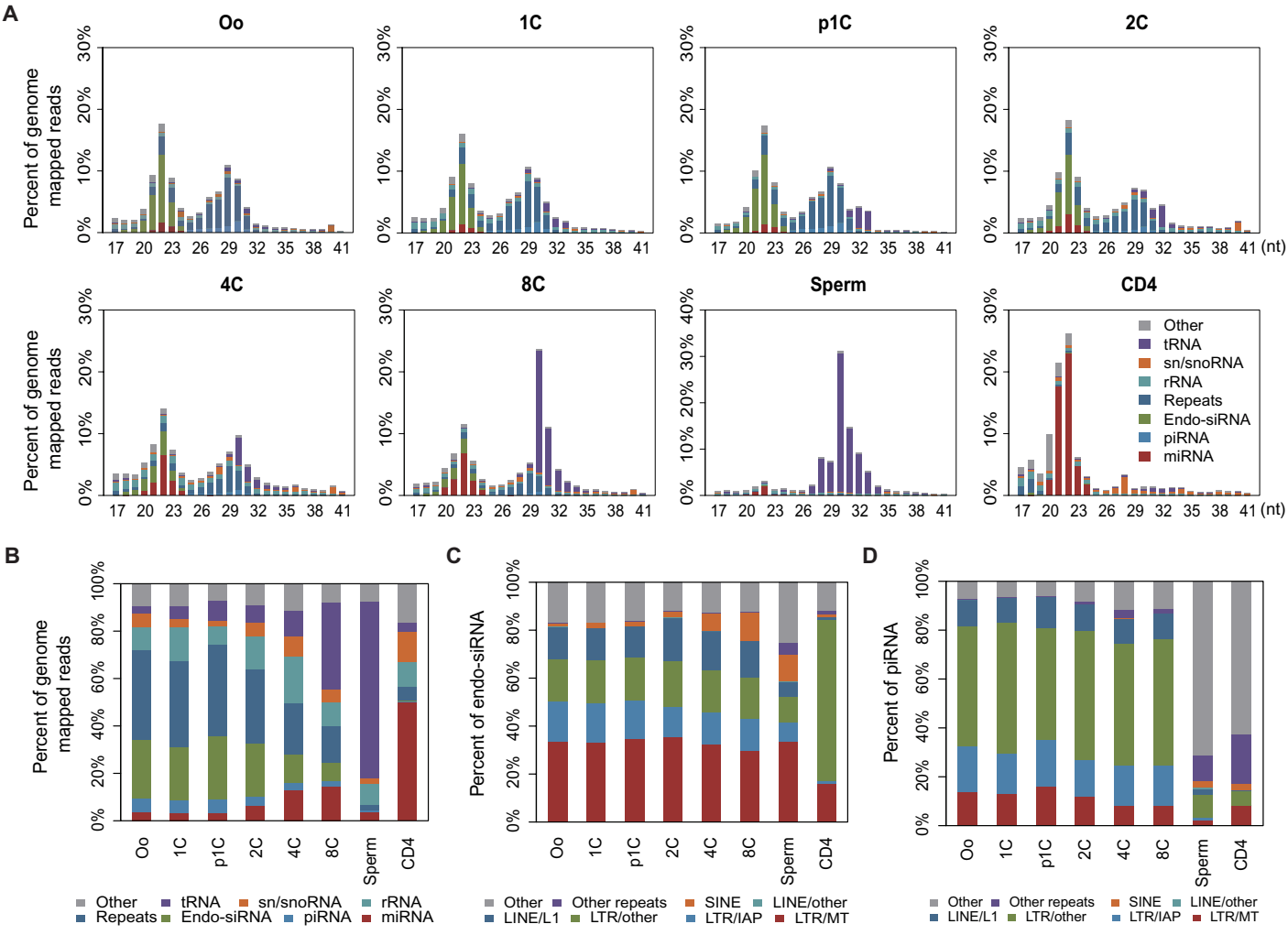

Fig. 2. Categories and length distributions of small RNAs. (**A**) Composition of small RNA categories according to their length distributions in each sample. (**B**) Percentage of different categories of small RNAs mapped onto the mouse genome in each developmental stage. Mouse CD4$^+$ T cell (CD4) sample serves as a somatic cell control. (**C** and **D**) Percentage of the endo-siRNAs (C) and piRNAs (D) derived from different types of repetitive elements. IAP, intracisternal A-particle; MT, mouse transcript.

initiated (*38*, *44*, *45*). Comparing the miRNA profiles of Oo, p1C, and 1C showed that miRNAs were expressed at almost identical levels ($R >$ 0.95) in those cells, suggesting that miRNAs in zygotes are mainly inherited from oocytes. Only 12 oocyte miRNAs were up-regulated by over twofold in 1C compared with p1C. Of these, five miRNAs, that is, miR-10a-5p, miR-34c-5p, miR-143-3p, miR-146a-5p, and miR-146b-5p, were highly expressed in the sperm (Fig. 4A). To further quantify the small RNAs carried into the zygote with sperm during fertilization, we performed qRT-PCR analysis of several abundant small RNAs in the oocytes and sperms (Fig. 4, B and C), including a glutamine tRNA (GluCTC) fragment, which was one of the most abundant small RNAs in sperm (*46*–*48*); miR-191, which was the most abundant miRNA in sperm; and miR-16 and miR-146a, which were highly expressed in sperm. By comparing the relative amounts of these small RNAs per oocyte or sperm, we found that the amount of processed small RNA carried by a single sperm was extremely low (<0.1%) compared with the amount already existing in an oocyte (Fig. 4C). This is expected because the cellular volume of an oocyte is hundreds of times greater than that of the sperm head. Although processed small RNAs are rarely carried into the oocyte by sperm, sperm-borne miRNAs may already be associated with AGO proteins and may function in early embryonic development through a RNA-induced silencing complex (RISC)–dependent or unknown noncanonical mechanism. Because we collected the zygotes right after pronucleus formation and a few hours before the initiation of transcription during minor ZGA (*31*, *38*, *44*, *45*), the miRNAs that were significantly up-regulated in zygotes are likely to be generated from the Drosha- and Dicer-mediated processing of miRNA precursors (pri-miRNA or pre-miRNA) that preexisted in the sperm or oocytes. This represents the first wave of miRNA expression in the zygotes. The production of miRNAs from the parentally inherited miRNA precursors in the zygote before genome activation implies that a new layer of posttranscriptional gene regulation is mediated by small RNAs during early embryonic development. The expression of these miRNAs continually increased with development (Fig. 4B), suggesting that these miRNA genes are transcriptionally activated in the later stages of development.

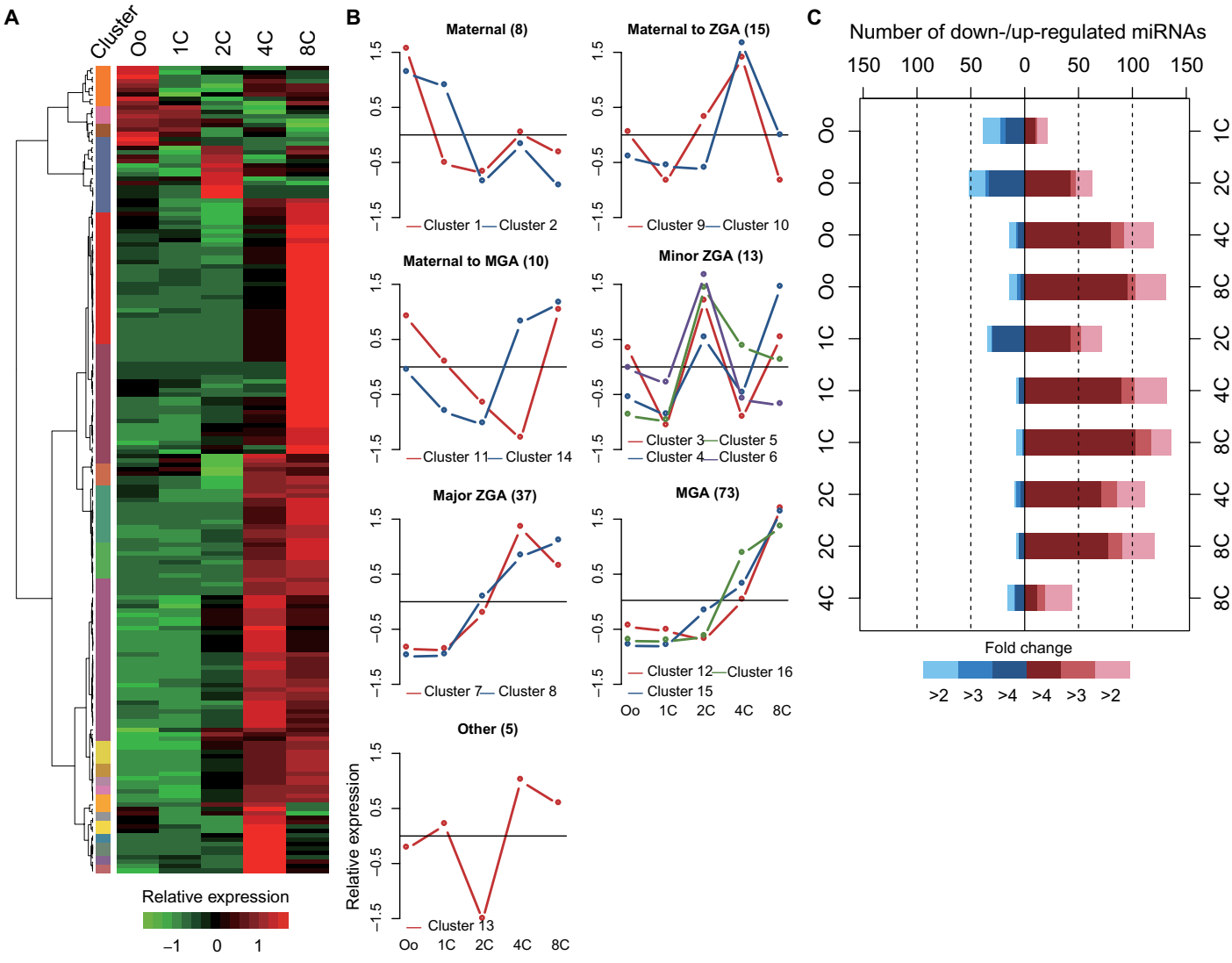

Fig. 3. Dynamic changes of miRNA expression in oocytes and early embryos. (**A**) Hierarchical clustering of normalized miRNA expression levels in Oo-8C. To characterize the change pattern, the expression of each miRNA from Oo to 8C was normalized using *Z* scores. The hierarchical tree was cut at an empirically defined height ($h = 0.4$) to characterize the maternal degradation and the MZT. (**B**) miRNAs were classified into seven groups according to their expression patterns. The number of miRNAs in each group is indicated in parentheses. (**C**) The numbers of differentially expressed miRNAs in all possible pairs of developmental stages. Blue and red bars represent down- and up-regulated miRNAs, respectively. Only miRNAs with RPM ≥20 and fold change ≥2 in at least one pair of adjacent stages are shown.

Extensive 3′ tailing of miRNAs and endo-siRNAs in early embryos

Posttranscriptional modifications of small RNAs include nucleotide editing, such as adenosine to inosine and cytidine to uridine (*49*–*51*), 2′-*O*-methyl modification, and addition of nontemplated nucleotides at the 3′ end (3′ tailing) (*52*–*54*). Despite their important functions, little is known about the small RNA modifications in mammalian early embryos. We found that the frequency of nucleotide editing of small RNAs in early embryos was low, less than 2% (table S1). The small RNAs tailed with nontemplated nucleotides were enriched at 20 to 23 nt, including miRNAs, endo-siRNAs, and ~22-nt fragments derived from repetitive elements (Fig. 5, A and B). By contrast, piRNAs, fragments derived from tRNAs and rRNAs (ribosomal RNAs), and ~29-nt fragments derived from repetitive elements had low levels of 3′ end nucleotide addition (Fig. 5B and fig. S2). This enrichment suggests that 3′ tailing is small RNA type–specific and may be caused by their associations with specific proteins, such as AGOs.

The frequency of small RNAs with 3′ tailing was significantly higher in early embryos than in later stages and in somatic cells. The nucleotide most commonly added to the 3′ end of miRNAs was adenosine (A), followed by uridine (U) (Fig. 5B and fig. S2). By contrast, additions of cytosine (C) or guanosine (G) were rare. It should be noted that the frequencies could be higher, considering that some of the last residue of small RNAs aligned to the genome were added through modifications.

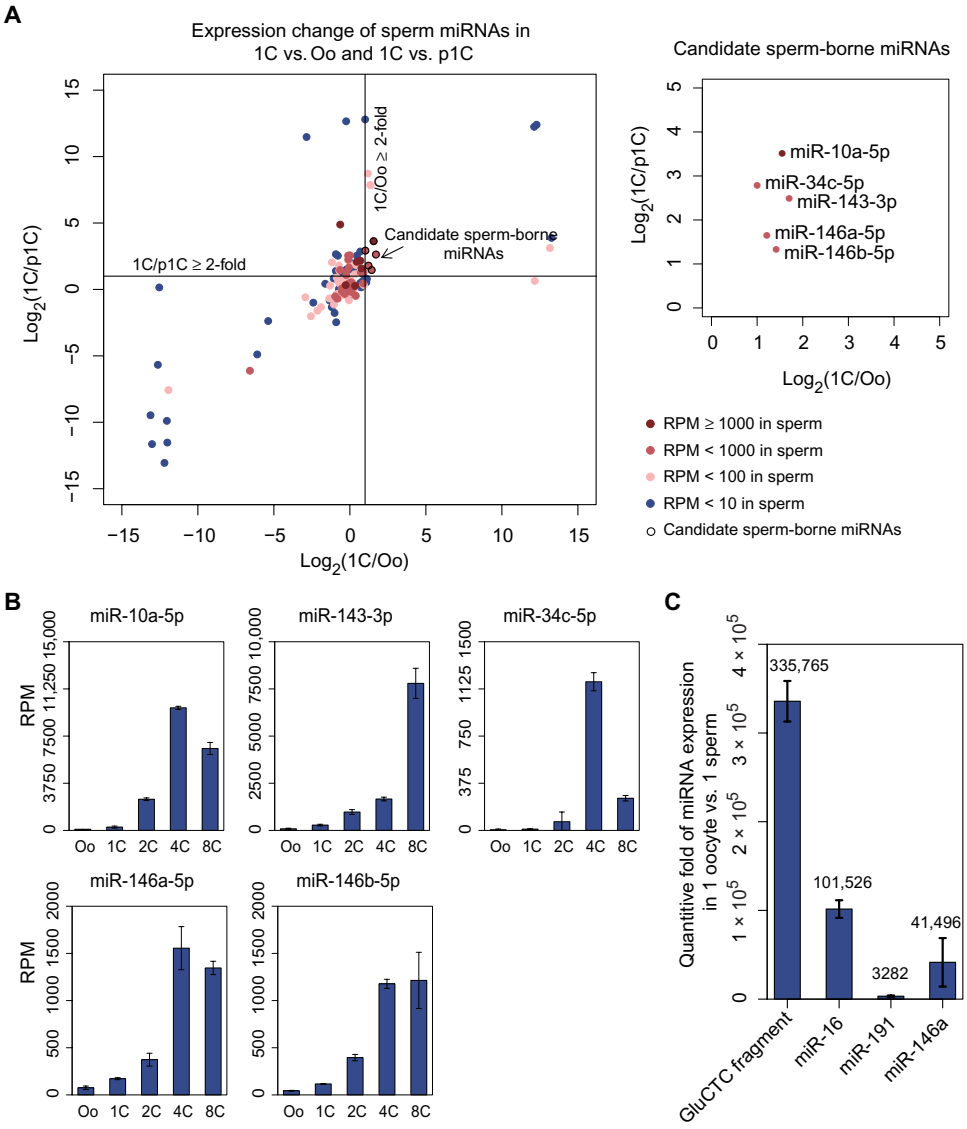

Fig. 4. The contribution of sperm-borne miRNAs to zygotic miRNAs. (**A**) Abundance changes of the potential sperm-borne miRNAs in 1C versus Oo and 1C versus p1C. The oocyte miRNAs that are increased significantly in 1C and p1C and highly expressed in sperm are marked with a black circle. (**B**) Expression level of above sperm-borne miRNA candidates in early developmental stages. (**C**) Relative abundance of a glutamine tRNA fragment and three miRNAs in an oocyte compared to that in a single sperm. The expression level of small RNAs in a single oocyte or sperm was quantified by qRT-PCR of a single oocyte or calculated by division by the number of sperms used for the qRT-PCR analyses. The assay was repeated at least three times independently.

In contrast to the similar level of adenylation for miRNAs and endo-siRNAs, uridylation of miRNAs was more frequent than that of endo-siRNAs, possibly due to the function of TUT proteins that adds uridine at the 3′ overhang of pre-miRNAs after Drosha/Dgcr8 cleavage (*55*). Unlike the single A tailing (monoadenylation) at the 3′ end of miRNAs that was often observed in somatic cells, miRNAs tailed with 2- to 4-As (oligoadenylation) were common in early embryos. The miRNA adenylation frequency was dynamically regulated during development, increasing by more than 50% in 1C and 2C and then decreasing rapidly by more than threefold in 4C and 8C, to a level comparable to that of somatic cells. Notably, this increase in the adenylation ratio during 1C-2C was mainly caused by oligoadenylation (Fig. 5B and fig. S2).

The adenylation frequency of individual miRNAs was highly variable despite the average level of 5 to 20%, with the maximum reaching ~80% (miR-92-1-3p at the 2C stage) (Fig. 5C, fig. S3A, and data set S1). Intriguingly, about half of the miRNA species did not contain 3′ A tailing during Oo-8C (Fig. 5, C and D), suggesting that adenylation is miRNA species–specific. However, no obvious sequence motif could be found using MEME (Multiple EM for Motif Elicitation) (*56*). We further ranked the miRNAs in a descending order based on the expression level of their canonical isomers and found that low-abundant miRNAs tended to be more highly adenylated in both embryonic and somatic cells (fig. S3B).

It has been reported that the addition of extra adenine at the 3′ end by GLD2 might stabilize miRNA (*57*–*59*). GLD2 is highly active in

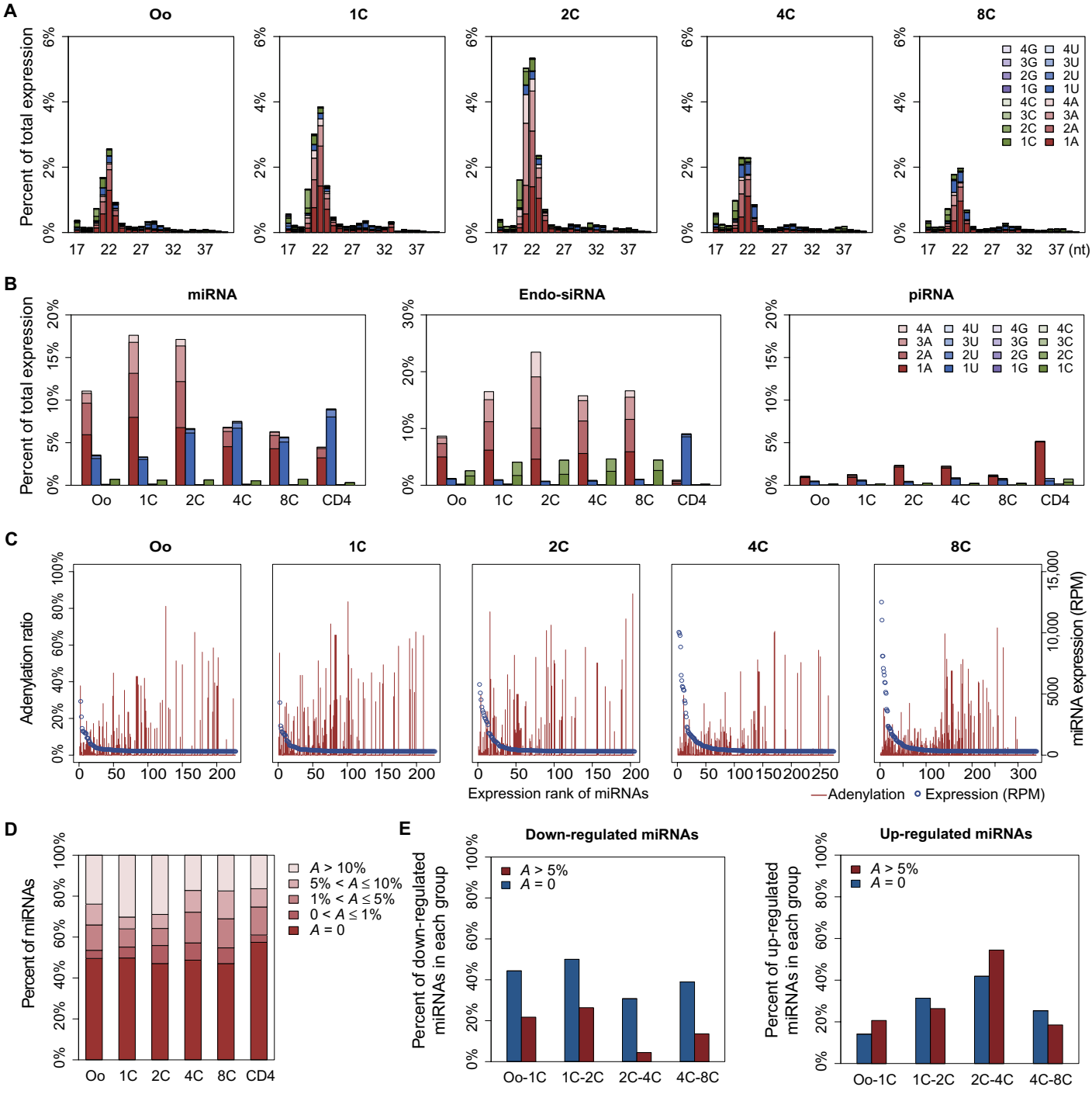

Fig. 5. 3′ tailing of small RNAs in oocytes and early embryos. (**A**) Length distribution of 3′ tailing ratio of small RNAs. Percentage of different-length small RNAs tailed with mono- and oligonucleotides in oocytes and early embryos. (**B**) Percentage of miRNA (left), endo-siRNA (middle), and piRNA (right) sequences tailed at 3′ end with mono- and oligonucleotides. (**C**) Adenylation ratio of individual miRNAs in each sample. The miRNAs are aligned from left to right according to their expression level from high to low. (**D**) Percentage of miRNAs with different adenylation (*A*) ratios in each sample. (**E**) Degradation of miRNAs with different adenylation ratios during early embryonic development. The percentage of down- (left) and up-regulated (right) miRNA species with low or high adenylation levels is calculated by comparing their abundance in adjacent stages.

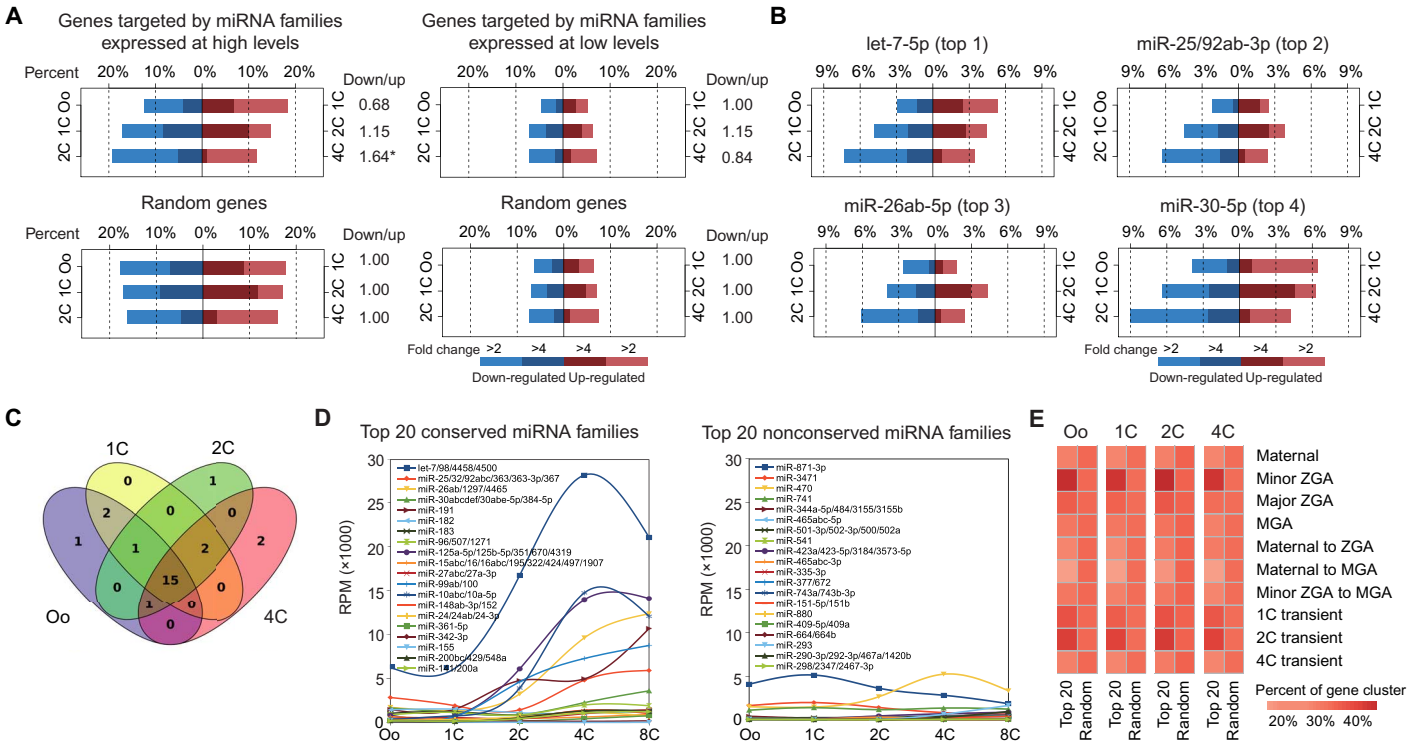

Fig. 6. Regulation of genes targeted by miRNAs in oocytes and early embryos. (**A**) Percentage of down- or up-regulated genes targeted by conserved miRNA families expressed at the highest (top 20, 100 < RPM) or lowest level (bottom 20, 0 < RPM < 10) in Oo-2C. Equal numbers of genes expressed in oocytes and embryos were selected randomly 1000 times to serve as a control (Random genes). Blue and red bars represent the percentage of down- and up-regulated genes, respectively. The number beside each bar indicates the relative ratio of the percentage of the down- and up-regulated genes. The asterisk represents that the relative ratio is significantly greater than Random genes ($P < 0.05$, Fisher's exact test). (**B**) Percentage of down- or up-regulated genes targeted by the most highly expressed conserved miRNA families in oocyte. (**C**) Overlap of the 20 most highly expressed conserved miRNA families expressed in Oo-4C. (**D**) Expression level of the 20 most highly expressed conserved (left) or nonconserved (right) miRNA families of oocytes in each stage. (**E**) Percentage of genes targeted by the 20 most abundant conserved miRNA families in each of the gene clusters identified previously. Randomly selected genes (Random) serve as control.

mammalian zygotes and well known for its role in the polyadenylation of mRNAs, which is critical for early embryonic development (*60*–*62*). However, a recent report showed that miRNA adenylation by wispy, a *Drosophila* homolog of GLD2, contributes to maternal miRNA degradation in the early embryonic development of *Drosophila* (*63*), a discrepancy that is likely due to the different species analyzed. Our deep sequencing data showed an obvious temporal increase in 3′ oligoadenylation, correlating with the time of the large-scale clearance of maternal miRNAs at the 1C and 2C stages (Figs. 3C and 5B), suggesting that the 3′ adenylation may facilitate or protect miRNAs from degradation. To distinguish these two opposite possibilities, we compared the decay rates of the two groups of miRNAs, adenylatable and nonadenylatable miRNA species, at adjacent stages. The percentage of nonadenylatable miRNAs undergoing degradation was significantly higher than that of adenylatable ones (Fig. 5E), suggesting that the nonadenylatable miRNAs are prone to faster degradation than the adenylatable ones. This observation supports the role of 3′ adenylation in protecting miRNAs from degradation, although we cannot exclude the possibility that the degradation mechanisms may be different for the nonadenylatable miRNAs and the nonadenylated portion of the adenylatable ones.

Repression and reactivation of miRNA function in early embryonic development

It was reported that miRNAs played important roles during MZT in zebrafish when the transcriptional landscape of embryos was reprogrammed (*26*). In mouse, approximately 65% of maternal mRNAs underwent significant degradation at the 1C-2C stages (*31*, *64*), an important regulatory event of gene expression during MZT. However, studies in mouse showed that miRNA functions were suppressed in oocytes and zygotes (*22*, *30*), raising the question regarding the role of miRNAs in maternal mRNA degradation. By integrating the conducted miRNA profiles of this study and the publicly available transcriptome profiles of embryos in the Oo-4C stages (*31*), we analyzed the genes targeted by the top 20 abundant and conserved miRNA families (RPM >200) in each adjacent stage as predicted by TargetScan. The number of up-regulated mRNAs approximately equaled that of the down-regulated ones targeted by miRNAs during the Oo-1C or 1C-2C stages (Fig. 6A), suggesting that miRNAs do not mediate the significant degradation of mRNAs during these periods, consistent with previous experimental results (*22*, *30*). To further investigate whether specific miRNAs could degrade maternal mRNAs as miR-430 does in zebrafish, we analyzed the targets of miR-430 homologs in mouse (miR-294/295-3p family) and other abundantly expressed conserved miRNA families in early embryos, respectively. Consistently, none of these miRNAs mediated the significant degradation of target mRNAs in Oo-1C or 1C-2C (Fig. 6B and fig. S4, A and B). These results indicate that the activity of miRNAs is repressed before the 2C stage, consistent with previous studies (*22*, *30*). Thus, miRNAs are unlikely to play an essential role in the clearance of maternal mRNAs during the MZT in mouse as

they do in zebrafish. This discrepancy may be because of the differences in the developmental stages used for analyzing maternal mRNA degradation. The period of mir-430 function in zebrafish is equivalent to the blastula stage in mouse, which is far beyond the period of MZT in mouse (*24*, *25*, *65*), although we cannot rule out the intrinsic differences in the mechanism of maternal RNA degradation because the embryogenesis of zebrafish is different from that of mammals. In any case, these findings suggest the existence of alternative mechanisms in initiating maternal mRNA clearance in mammalian early embryos (*24*, *25*, *65*).

A previous study showed that the development of the DGCR8 knockout mouse was arrested at E6.5 (*66*), suggesting that miRNAs are essential for early embryonic development despite repression of their activity in oocytes and stage 1C. Therefore, to explore the restoration times of miRNA functions is of great interest. We observed a significant degradation of mRNAs predicted to be targeted by the top 20 highly expressed, conserved miRNA families, both collectively ($P = 3.3 \times 10^{-8}$, Fisher's exact test) in 2C-4C (Fig. 6A) and individually (fig. S4B). In contrast, no such trend was observed for the miRNA families that were expressed at a low level ($0 < RPM < 10$), consistent with the dependency of miRNA expression level for their functions (*67*). These observations suggest that the repression activity of the miRNA is switched on approximately at the 2C stage and increases gradually at later stages. Such a transition may be induced by the expression or reactivation of RISC components, such as AGOs and GW182, in early embryos (*68*–*70*).

The miRNA targets down-regulated in the 2C-4C stages were enriched with pivotal genes in the signaling pathways of stem cell pluripotency maintenance, including *Lin28*, *Stat3*, *APC*, and *Nras* (fig. S5, A and B, and data set S2). Tet3, an enzyme that catalyzes the key step in DNA demethylation during early embryonic development (*71*), was also predicted to be targeted by several of the most abundant oocyte miRNAs, including Let-7, miR-26a/b, and miR-125a/b (fig. S5B). These results indicate that the regulatory function of miRNAs is reactivated to repress important stemness genes after the 2C stage, thus promoting the development of embryos, an observation worth investigating in the future.

Although many maternal miRNAs underwent extensive degradation, the composition of the top 20 highly expressed, conserved miRNA families in Oo-4C was very similar (Fig. 6C). Intriguingly, more than half of them, including Let-7, miR-191, and miR-125a/b, were also actively produced in early embryos, resulting in a continuous increase in their abundance during development (Fig. 6D). In contrast, no such up-regulation was observed for most of the nonconserved maternal miRNAs, despite some of them also being quite abundant in oocytes (Fig. 6D). Moreover, significantly more genes that were transiently expressed in 2C (minor ZGA and 2C transient) were down-regulated by these abundant and conserved miRNA families in the oocytes (Fig. 6E). These findings suggest that, in addition to their roles in oogenesis, maternal miRNAs appear to have important functions in early embryonic development. It may be that they are stored in the mature oocyte with their activity being repressed to avoid disturbing the gene expression in minor ZGA and are reactivated after the 2C stage to regulate early zygotic genes posttranscriptionally along with their newly produced siblings.

MATERIALS AND METHODS

Animal use and care

All animal procedures were performed in compliance with the guidelines of the Shanghai Institute of Biochemistry and Cell Biology, Shanghai Institutes for Biological Sciences, Chinese Academy of Sciences.

Collection of oocytes and early embryos

Female FVB/N mice (8 to 12 weeks old) were superovulated via intraperitoneal injection of 10 IU of pregnant mare serum gonadotropin and 10 IU of human chorionic gonadotropin (hCG) at 46- to 48-hour intervals. Cumulus-oocyte complexes were collected from the oviducts 13 to 15 hours later and treated with bovine testicular hyaluronidase (1 mg/ml) (Sigma-Aldrich) for 1 to 2 min. Cumulus-free high-quality oocytes [metaphase II (MII)] were then collected. For the collection of fertilized embryos, female mice were mated with male FVB/N mice after hCG injection and inspected for vaginal plugs within 15 hours. Pronucleus stage 1C embryos, 2C embryos, and 4C embryos were isolated from the oviducts of plug-positive female mice at 18, 40, and 60 hours, respectively, after hCG injection. Eight-cell embryos were collected from oviducts and uteri at 68 to 70 hours after hCG injection. To obtain the early pronucleus–stage parthenogenetic embryos, MII oocytes were parthenogenetically activated by culturing in KCl-enriched simplex optimized medium (KSOM, Millipore) containing 10 mM $SrCl_2$, 4 mM EGTA, and cytochalasin B (5 μg/ml) for 6 hours. The stage of the oocytes and embryos was visually inspected under a microscope. All oocytes and embryos were washed thrice in cold Dulbecco's phosphate-buffered saline (DPBS) containing 0.01% polyvinyl alcohol and stored in TRIzol Reagent (Ambion) at −80°C.

Collection of mouse sperms

Epididymides were collected from male FVB/N mice aged 10 to 12 weeks. After epididymal ducts were cut with sharp scissors, a lump of the dense sperm mass was placed in 1 ml of human tubal fluid (HTF) medium and incubated at 37°C for 10 min in a 0.5% CO_2 atmosphere. The sperm was then purified by Percoll gradient centrifugation. Sperm suspension at 1 ml was loaded onto a two-step Percoll gradient (40 and 80% Percoll in HTF), followed by centrifugation at 380*g* for 20 min, and then the two top layers were removed. The sperm pellet was washed twice with DPBS before being harvested and counted with a cell counting chamber. Aliquots of sperm were stored in 500 μl of TRIzol Reagent (Ambion) at −80°C.

Preparing cDNA library of small RNAs for deep sequencing

cDNA libraries of small RNAs were constructed using HEK293 total RNA, with threefold serial dilutions ranging from 100 to 1 ng. For mouse oocyte and embryo samples, total RNA was extracted from 111 MII oocytes, 167 1C embryos, 137 2C embryos, 57 4C embryos, 102 8C embryos, 200 p1C embryos, or ~3×10^6 sperms using TRIzol Reagent (Ambion) containing 45 μM $MgCl_2$ (*72*), respectively. The quantity of isolated RNA was measured with Qubit 2.0 Fluorometer (Invitrogen). Each cDNA library of small RNAs was constructed using 10 ng of total RNA with two technical replicates.

Adaptor ligation. Total RNA (10 ng) was mixed with 0.25 pmol 3′ adapter, 1× T4 ligase reaction buffer, 33% polyethylene glycol (molecular weight 8000), 40 U RNL2tr K227Q (NEB), and 20 U RiboLock RNase Inhibitor (Thermo Fisher Scientific) in a 10-μl reaction volume. The samples were incubated at 22°C for 2 hours, followed by an addition of 1 μl of 5 μM RT primer before heat inactivation at 75°C for 5 min. The total ligation products were used for 5′ adapter ligation in a 14.5-μl reaction containing 5 pmol of 5′ adapter, 10 μmol of adenosine triphosphate (ATP), 10 U of T4 RNA ligase 1 (NEB), and 20 U of RiboLock

RNase inhibitor (Thermo Fisher Scientific) and then incubated at 22°C for 1 hour.

First-strand cDNA synthesis. Ligation product (10 μl) was used as a template in a final 20-μl RT reaction containing 200 U of M-MuLV Reverse Transcriptase (NEB), 1× RT reaction buffer, 10 mM dithiothreitol, 2.5 μmol of deoxynucleotide triphosphate (dNTP) each, and 20 U of RiboLock RNase inhibitor (Thermo Fisher Scientific). The RT reaction was performed at 44°C for 1 hour.

PCR amplification. The RT product was amplified by high-fidelity DNA polymerase as follows: 50-μl reaction containing 5 μl of RT reaction product, 1 U of KOD-Plus- Neo (TOYOBO), 1× PCR buffer, 25 pmol of RP1 primer, 25 pmol of RPI pimer, 1.5 mM $MgSO_4$, 0.2 mM each dNTP, and H_2O. The PCR mixture was heated to 94°C for 2 min, followed by 22 cycles at 98°C for 10 s, 60°C for 30 s, and 68°C for 15 s.

Gel purification. RT-PCR products were separated on a 6% polyacrylamide gel and visualized using GeneGreen dye (TIANGEN). The 130– to 160–base pair (bp) DNA fragments corresponding to the small RNA fraction were cut off from the gel. The gel piece was smashed, and DNA was eluted in TE buffer [10 mM tris (pH 7.5) and 1 mM EDTA] overnight with rotation at room temperature. The liquid phase was passed through a 0.45-μm Spin-X column (Corning), followed by precipitation with 10 μg of linear acrylamide, $^1/_{10}$ volume of 3 M sodium acetate (pH 5.2), and three volumes of ethanol.

Sequencing. For the sequencing of small RNA libraries, an Illumina HiSeq 2000 sequencer was used. The sequencing data were deposited in the Sequence Read Archive (accession no. SRP045287).

Real-time qRT-PCR of small RNAs

Single-oocyte, zygote, or 1-ng sperm total RNA was used for RT by following a previously described method (*73*). Equal amounts of a synthetic siRNA, siEGFP, were added into each sample as a spike-in control. The sperm was collected as described above, and the number of sperms was counted before RNA extraction. The amount of RNA obtained from a single sperm was calculated by dividing the total RNA yield by the input sperm number.

In each RNA sample from human cell lines, 1×10^{-5} pmol of siEGFP was spiked into each microgram of total RNA. The RNA was used for polyadenylate [poly(A)] addition and RT-PCR analyses as previously described (*74*). Two micrograms of total RNA was polyadenylated by incubation with 1 mM ATP and 1.25 U of poly(A) polymerase (NEB) at 37°C for 30 min in a 20-μl reaction mixture. After treatment with 1 U deoxyribonuclease I (Thermo Fisher Scientific) at 37°C for 15 min, the RNA was denatured in the presence of 2.5 mM EDTA at 70°C for 10 min and snap-cooled on ice. Five hundred nanograms of RNA was reverse-transcribed with 200 U of M-MLV Reverse Transcriptase (TAKARA) and 1 μM oligo(dT) according to the manufacturer's instructions. Real-time PCR was performed with a StepOnePlus real-time PCR machine (Applied Biosystems) and SYBR Green reagent (Roche). The cycling conditions were 95°C for 10 min and 40 cycles of 95°C for 10 s and 60°C for 30 s.

Comparing the relative expression of miRNA in different cell lines

Nine miRNAs that have no or few isoforms (to avoid cross-amplification during RT-PCR) were randomly selected to validate the relative expression levels determined by small RNA sequencing and qRT-PCR (see Supplementary Materials and Methods). $miR_{i,a}$ represents the expression of miRNA *i* in the cell line *a*. $miR_{i,a}/miR_{j,a}$ represents the relative expression of miR_i and miR_j in the cell line *a*. The ratio of the relative expression of miR_i and miR_j in cell lines *a* and *b* was calculated using the equation $(cell_a/cell_b)_{i,j} = (miR_{i,a}/miR_{j,a})/(miR_{i,b}/miR_{j,b})$ and is shown in fig. S1 (B and C).

Analyses of small RNA expression

Read sequences longer than 17 nt after adapter trimming were used for mapping to the libraries of miRNAs, tRNAs, rRNAs, sn/snoRNAs (small nuclear/small nucleolar RNAs), endo-siRNA, piRNAs, and repetitive elements sequentially.

Mapping of miRNAs

The miRNA expression level was determined on the basis of the number of reads that was mapped to the annotated miRNA sequences in miRBase version 21, allowing −2 or +2 nt to be templated by the corresponding genomic sequence at the 3′ end (http://www.mirbase.org/). Normalization was performed by dividing the read counts of the individual miRNA by the total number of reads mapped to the mouse genome and presented as RPM.

Mapping of endo-siRNA, piRNA, and other small RNAs

Previously annotated endo-siRNA libraries (*15*–*17*) were combined with the endo-siRNAs identified by our in-house program. The prediction of endo-siRNAs was performed as follows: The mouse genome sequence was scanned in 5-kb windows to find regions that had more than five uniquely mapped small RNAs of 18 to 24 nt. The cluster boundaries of potential endo-siRNA clusters were defined by the location of the 5′ and 3′ distal small RNAs. Then, Exonerate was used to extract regions of >100 bp with significant cis- and trans-transcript pairing. Hairpin structure was predicted by RNAFold. If >80% read counts of the small RNAs mapped into these regions were between 18 and 24 nt (to exclude piRNA clusters) and both the sense and antisense reads were present, then this cluster was categorized as a putative endo-siRNA cluster. The small RNAs of 18 to 24 nt mapped into these endo-siRNA clusters were characterized as endo-siRNAs. The expression of piRNA was calculated by mapping the reads to the previously annotated piRNA libraries from four databases: piRNABank (http://pirnabank.ibab.ac.in/), RNA database (http://jsm-research.imb.uq.edu.au/rnadb), the Gene Expression Omnibus database (GSE7414), and GenBank (ftp://ftp.ncbi.nih.gov/genbank/). To identify other repetitive element–derived small RNAs, small RNAs that did not belong to the piRNA and endo-siRNA libraries were aligned to the consensus sequences of transposable elements, such as LINE, SINE (short interspersed nuclear element), and DNA transposon, from the Web site of University of California Santa Cruz (UCSC) Genome Bioinformatics (http://hgdownload.cse.ucsc.edu/downloads.html). The database for mapping the small RNAs derived from tRNAs, rRNAs, and sn/snoRNAs was downloaded from the following databases: tRNAs from the Genomic tRNA Database (http://lowelab.ucsc.edu/GtRNAdb) and rRNAs and sn/snoRNAs from Ensembl Genes (www.ensembl.org). The relative abundance of these small RNAs, including reads with 3′ tailing, was calculated and presented as RPM.

Analyses of 3′ tailing of small RNAs

Besides the reads that could be perfectly mapped to the mouse genome, we also collected those with nontemplated nucleotide addition at their 3′ end. The total expression of each small RNA was calculated by adding the count of perfectly matched reads and those with 3′ tailing. The ratio of nontemplated 3′ tailing was defined as the proportion

of the 3′ tailed read count over the total read count. The ratio of miRNA tailing might be underestimated because the last residue of some small RNAs aligned to the genome was added through modifications. Only the miRNAs that expressed >1 RPM were used for the investigation of the influence of 3′ adenylation on miRNA stability.

Target gene prediction and functional annotation of miRNA families

The annotations of miRNA families and their targets were downloaded from TargetScan (www.targetscan.org/mmu_61/). To minimize the false-positive prediction of miRNA targets, only conserved miRNA families and their conserved targets were used for our functional annotation. The genes targeted by both high (100 < RPM) and low (0 < RPM < 10) abundant miRNA families were not included in the comparison in Fig. 6A because the highly expressed miRNA families may have a dominant contribution to the down-regulation of the targeted gene as compared to those expressed at a low level. To investigate the biological processes potentially influenced by miRNAs, the enrichment of their differentially expressed target genes in KEGG (Kyoto Encyclopedia of Genes and Genomes) pathways (www.genome.jp/kegg/pathway.html) was calculated with Fisher's exact test.

SUPPLEMENTARY MATERIALS

Supplementary material for this article is available at http://advances.sciencemag.org/cgi/content/full/2/6/e1501482/DC1

fig. S1. Reproducibility of the deep sequencing method and comparison with the qRT-PCR method.

fig. S2. Percentage of 3′ mono- and oligonucleotides tailing of different type small RNAs in early embryos.

fig. S3. Adenylation ratio and expression level of miRNAs.

fig. S4 Percentage of down- or up-regulated genes targeted by individual miRNA families.

fig. S5. Predicted pluripotency genes regulated by the highly expressed conserved miRNA families during early embryonic development.

table S1. miRNA editing ratio in oocyte and early zygotic stages.

Sequence information of oligonucleotides

data set S1. Expression level and adenylation ratio of miRNAs, endo-siRNAs, piRNAs, and tRNA-derived fragments in mouse oocytes and embryos.

data set S2. Down-regulated genes targeted by the conserved 20 most abundant miRNA families in 2C-4C embryos.

REFERENCES AND NOTES

1. L. He, G. J. Hannon, MicroRNAs: Small RNAs with a big role in gene regulation. *Nat. Rev. Genet.* **5**, 522–531 (2004).
2. D. P. Bartel, MicroRNAs: Genomics, biogenesis, mechanism, and function. *Cell* **116**, 281–297 (2004).
3. E. Bernstein, A. A. Caudy, S. M. Hammond, G. J. Hannon, Role for a bidentate ribonuclease in the initiation step of RNA interference. *Nature* **409**, 363–366 (2001).
4. V. N. Kim, MicroRNA biogenesis: Coordinated cropping and dicing. *Nat. Rev. Mol. Cell Biol.* **6**, 376–385 (2005).
5. W. P. Kloosterman, R. H. A. Plasterk, The diverse functions of microRNAs in animal development and disease. *Dev. Cell* **11**, 441–450 (2006).
6. E. Huntzinger, E. Izaurralde, Gene silencing by microRNAs: Contributions of translational repression and mRNA decay. *Nat. Rev. Genet.* **12**, 99–110 (2011).
7. K. Okamura, E. C. Lai, Endogenous small interfering RNAs in animals. *Nat. Rev. Mol. Cell Biol.* **9**, 673–678 (2008).
8. A. A. V. Albertini A. K. Wernimont, T. Muziol, R. B. G. Ravelli, C. R. Clapier, G. Schoehn, W. Weissenhorn, R. W. H. Ruigrok, Crystal structure of the rabies virus nucleoprotein-RNA complex. *Science* **313**, 360–363 (2006).
9. A. Aravin, D. Gaidatzis, S. Pfeffer, M. Lagos-Quintana, P. Landgraf, N. Iovino, P. Morris, M. J. Brownstein, S. Kuramochi-Miyagawa, T. Nakano, M. Chien, J. J. Russo, J. Ju, R. Sheridan, C. Sander, M. Zavolan, T. Tuschl, A novel class of small RNAs bind to MILI protein in mouse testes. *Nature* **442**, 203–207 (2006).
10. A. Girard, R. Sachidanandam, G. J. Hannon, M. A. Carmell, A germline-specific class of small RNAs binds mammalian Piwi proteins. *Nature* **442**, 199–202 (2006).
11. M. A. Carmell, A. Girard, H. J. G. van de Kant, D. Bourc'his, T. H. Bestor, D. G. de Rooij, G. J. Hannon, MIWI2 is essential for spermatogenesis and repression of transposons in the mouse male germline. *Dev. Cell* **12**, 503–514 (2007).
12. W. Deng, H. Lin, *miwi*, a murine homolog of *piwi*, encodes a cytoplasmic protein essential for spermatogenesis. *Dev. Cell* **2**, 819–830 (2002).
13. S. Kuramochi-Miyagawa T. Kimura, T. W. Ijiri, T. Isobe, N. Asada, Y. Fujita, M. Ikawa, N. Iwai, M. Okabe, W. Deng, H. Lin, Y. Matsuda, T. Nakano, *Mili*, a mammalian member of *piwi* family gene, is essential for spermatogenesis. *Development* **131**, 839–849 (2004).
14. T. Watanabe, H. Lin, Posttranscriptional regulation of gene expression by Piwi proteins and piRNAs. *Mol. Cell* **56**, 18–27 (2014).
15. O. H. Tam, A. A. Aravin, P. Stein, A. Girard, E. P. Murchison, S. Cheloufi, E. Hodges, M. Anger, R. Sachidanandam, R. M. Schultz, G. J. Hannon, Pseudogene-derived small interfering RNAs regulate gene expression in mouse oocytes. *Nature* **453**, 534–538 (2008).
16. T. Watanabe, Y. Totoki, A. Toyoda, M. Kaneda, S. Kuramochi-Miyagawa, Y. Obata, H. Chiba, Y. Kohara, T. Kono, T. Nakano, M. A. Surani, Y. Sakaki, H. Sasaki, Endogenous siRNAs from naturally formed dsRNAs regulate transcripts in mouse oocytes. *Nature* **453**, 539–543 (2008).
17. Y. Ohnishi, Y. Totoki, A. Toyoda, T. Watanabe, Y. Yamamoto, K. Tokunaga, Y. Sakaki, H. Sasaki, H. Hohjoh, Small RNA class transition from siRNA/piRNA to miRNA during pre-implantation mouse development. *Nucleic Acids Res.* **38**, 5141–5151 (2010).
18. F. Tang, M. Kaneda, D. O'Carroll, P. Hajkova, S. C. Barton, Y. A. Sun, C. Lee, A. Tarakhovsky, K. Lao, M. A. Surani, Maternal microRNAs are essential for mouse zygotic development. *Genes Dev.* **21**, 644–648 (2007).
19. M. Kaneda, F. Tang, D. O'Carroll, K. Lao, M. A. Surani, Essential role for Argonaute2 protein in mouse oogenesis. *Epigenetics Chromatin* **2**, 9 (2009).
20. E. P. Murchison, P. Stein, Z. Xuan, H. Pan, M. Q. Zhang, R. M. Schultz, G. J. Hannon, Critical roles for Dicer in the female germline. *Genes Dev.* **21**, 682–693 (2007).
21. P. Stein, N. V. Rozhkov, F. Li, F. L. Cárdenas, O. Davydenk, L. E. Vandivier, B. D. Gregory, G. J. Hannon, R. M. Schultz, Essential role for endogenous siRNAs during meiosis in mouse oocytes. *PLOS Genet.* **11**, e1005013 (2015).
22. N. Suh, L. Baehner, F. Moltzahn, C. Melton, A. Shenoy, J. Chen, R. Blelloch, MicroRNA function is globally suppressed in mouse oocytes and early embryos. *Curr. Biol.* **20**, 271–277 (2010).
23. E. Bernstein, E. Bernstein, S. Y. Kim, M. A. Carmell, E. P. Murchison, H. Alcorn, M. Z. Li, A. A. Mills, S. J. Elledge, K. V. Anderson, G. J. Hannon, Dicer is essential for mouse development. *Nat. Genet.* **35**, 215–217 (2003).
24. W. Tadros, H. D. Lipshitz, The maternal-to-zygotic transition: A play in two acts. *Development* **136**, 3033–3042 (2009).
25. C. B. Walser, H. D. Lipshitz, Transcript clearance during the maternal-to-zygotic transition. *Curr. Opin. Genet. Dev.* **21**, 431–443 (2011).
26. A. J. Giraldez, Y. Mishima, J. Rihel, R. J. Grocock, S. Van Dongen, K. Inoue, A. J. Enright, A. F. Schier, Zebrafish MiR-430 promotes deadenylation and clearance of maternal mRNAs. *Science* **312**, 75–79 (2006).
27. E. Lund, M. Liu, R. S. Hartley, M. D. Sheets, J. E. Dahlberg, Deadenylation of maternal mRNAs mediated by miR-427 in *Xenopus laevis* embryos. *RNA* **15**, 2351–2363 (2009).
28. J. M. Calabrese, A. C. Seila, G. W. Yeo, P. A. Sharp, RNA sequence analysis defines Dicer's role in mouse embryonic stem cells. *Proc. Natl. Acad. Sci. U.S.A.* **104**, 18097–18102 (2007).
29. L. A. Medeiros, L. M. Dennis, M. E. Gill, H. Houbaviy, S. Markoulaki, D. Fu, A. C. White, O. Kirak, P. A. Sharp, D. C. Page, R. Jaenisch, *Mir-290–295* deficiency in mice results in partially penetrant embryonic lethality and germ cell defects. *Proc. Natl. Acad. Sci. U.S.A.* **108**, 14163–14168 (2011).
30. J. Ma, M. Flemr, P. Stein, P. Berninger, R. Malik, M. Zavolan, P. Svoboda, R. M. Schultz, MicroRNA activity is suppressed in mouse oocytes. *Curr. Biol.* **20**, 265–270 (2010).
31. S.-J. Park, M. Komata, F. Inoue, K. Yamada, K. Nakai, M. Ohsugi, K. Shirahige, Inferring the choreography of parental genomes during fertilization from ultralarge-scale whole-transcriptome analysis. *Genes Dev.* **27**, 2736–2748 (2013).
32. C. Malone, J. Brennecke, B. Czech, A. Aravin, G. J. Hannon, Preparation of small RNA libraries for high-throughput sequencing. *Cold Spring Harb. Protoc.* **2012**, 1067–1077(2012).
33. S. Kuramochi-Miyagawa, T. Watanabe, K. Gotoh, Y. Totoki, A. Toyoda, M. Ikawa, N. Asada, K. Kojima, Y. Yamaguchi, T. W. Ijiri, K. Hata, E. Li, Y. Matsuda, T. Kimura, M. Okabe, Y. Sakaki, H. Sasaki, T. Nakano, DNA methylation of retrotransposon genes is regulated by Piwi family members MILI and MIWI2 in murine fetal testes. *Genes Dev.* **22**, 908–917 (2008).
34. H. Goodarzi, X. Liu, H. C. B. Nguyen, S. Zhang, L. Fish, S. F. Tavazoie, Endogenous tRNA-derived fragments suppress breast cancer progression via YBX1 displacement. *Cell* **161**, 790–802 (2015).
35. Q. Chen, M. Yan, Z. Cao, X. Li, Y. Zhang, J. Shi, G.-H. Feng, H. Peng, X. Zhang, Y. Zhang, J. Qian, E. Duan, Q. Zhai, Q. Zhou, Sperm tsRNAs contribute to intergenerational inheritance of an acquired metabolic disorder. *Science* **351**, 397–400 (2015).
36. U. Sharma, C. C. Conine, J. M. Shea, A. Boskovic, A. G. Derr, X. Y. Bing, C. Belleannee, A. Kucukural, R. W. Serra, F. Sun, L. Song, B. R. Carone, E. P. Ricci, X. Z. Li, L. Fauquier, M. J. Moore, R. Sullivan, C. C. Mello, M. Garber, O. J. Rando, Biogenesis and function of

tRNA fragments during sperm maturation and fertilization in mammals. *Science* **351**, 391–396 (2015).
37. Y. Yang, W. Bai, L. Zhang, G. Yin, X. Wang, J. Wang, H. Zhao, Y. Han, Y.-Q. Yao, Determination of microRNAs in mouse preimplantation embryos by microarray. *Dev. Dyn.* **237**, 2315–2327 (2008).
38. C. Bouniol, E. Nguyen, P. Debey, Endogenous transcription occurs at the 1-cell stage in the mouse embryo. *Exp. Cell Res.* **218**, 57–62 (1995).
39. H. Wang, S. K. Dey, Roadmap to embryo implantation: Clues from mouse models. *Nat. Rev. Genet.* **7**, 185–199 (2006).
40. K. Gapp, A. Jawaid, P. Sarkies, J. Bohacek, P. Pelczar, J. Prados, L. Farinelli, E. Miska, I. M. Mansuy, Implication of sperm RNAs in transgenerational inheritance of the effects of early trauma in mice. *Nat. Neurosci.* **17**, 667–669 (2014).
41. O. Rechavi, L. Houri-Ze'evi, S. Anava, W. S. S. Goh, S. Y. Kerk, G. J. Hannon, O. Hobert, Starvation-induced transgenerational inheritance of Small RNAs in *C. elegans*. *Cell* **158**, 277–287 (2014).
42. W.-M. Liu, R. T. K. Pang, P. C. N. Chiu, B. P. C. Wong, K. Lao, K.-F. Lee, W. S. B. Yeung, Sperm-borne microRNA-34c is required for the first cleavage division in mouse. *Proc. Natl. Acad. Sci. U.S.A.* **109**, 490–494 (2012).
43. S. Yuan, C. Tang, Y. Zhang, J. Wu, J. Bao, H. Zheng, C. Xu, W. Yan, mir-34b/c and mir-449a/b/c are required for spermatogenesis, but not for the first cleavage division in mice. *Biol. Open* **4**, 212–223 (2015).
44. F. Aoki, D. M. Worrad, R. M. Schultz, Regulation of transcriptional activity during the first and second cell cycles in the preimplantation mouse embryo. *Dev. Biol.* **181**, 296–307 (1997).
45. K. Matsumoto, M. Anzai, N. Nakagata, A. Takahashi, Y. Takahashi, K. Miyata, Onset of paternal gene activation in early mouse embryos fertilized with transgenic mouse sperm. *Mol. Reprod. Dev.* **39**, 136–140 (1994).
46. C. Cole, A. Sobala, C. Lu, S. R. Thatcher, A. Bowman, J. W. S. Brown, P. J. Green, G. J. Barton, G. Hutvagner, Filtering of deep sequencing data reveals the existence of abundant Dicer-dependent small RNAs derived from tRNAs. *RNA* **15**, 2147–2160 (2009).
47. Y. S. Lee, Y. Shibata, A. Malhotra, A. Dutta, A novel class of small RNAs: tRNA-derived RNA fragments (tRFs). *Genes Dev.* **23**, 2639–2649 (2009).
48. H. Peng, J. Shi, Y. Zhang, H. Zhang, S. Liao, W. Li, L. Lei, C. Han, L. Ning, Y. Cao, Q. Zhou, Q. Chen, E. Duan, A novel class of tRNA-derived small RNAs extremely enriched in mature mouse sperm. *Cell Res.* **22**, 1609–1612 (2012).
49. A. Athanasiadis, A. Rich, S. Maas, Widespread A-to-I RNA editing of Alu-containing mRNAs in the human transcriptome. *PLOS Biol.* **2**, e391 (2004).
50. A. Jarmuz, A. Chester, J. Bayliss, J. Gisbourne, I. Dunham, J. Scott, N. Navaratnam, An anthropoid-specific locus of orphan C to U RNA-editing enzymes on chromosome 22. *Genomics* **79**, 285–296 (2002).
51. E. Y. Levanon, E. Eisenberg, R. Yelin, S. Nemzer, M. Hallegger, R. Shemesh, Z. Y. Fligelman, A. Shoshan, S. R. Pollock, D. Sztybel, M. Olshansky, G. Rechavi, M. F. Jantsch, Systematic identification of abundant A-to-I editing sites in the human transcriptome. *Nat. Biotechnol.* **22**, 1001–1005 (2004).
52. Y.-K. Kim, I. Heo, V. N. Kim, Modifications of small RNAs and their associated proteins. *Cell* **143**, 703–709 (2010).
53. C. T. Neilsen, G. J. Goodall, C. P. Bracken, IsomiRs–The overlooked repertoire in the dynamic microRNAome. *Trends Genet.* **28**, 544–549 (2012).
54. B. Yu, Z. Yang, J. Li, S. Minakhina, M. Yang, R. W. Padgett, R. Steward, X. Chen, Methylation as a crucial step in plant microRNA biogenesis. *Science* **307**, 932–935 (2005).
55. I. Heo, C. Joo, J. Cho, M. Ha, J. Han, V. Narry Kim, Lin28 mediates the terminal uridylation of let-7 precursor microRNA. *Mol. Cell* **32**, 276–284 (2008).
56. T. L. Bailey, J. Johnson, C. E. Grant, W. S. Noble, The MEME suite. *Nucleic Acids Res.* **43**, W39–W49 (2015).
57. A. D'Ambrogio, W. Gu, T. Udagawa, C. C. Mello, J. D. Richter, Specific miRNA stabilization by Gld2-catalyzed monoadenylation. *Cell Rep.* **2**, 1537–1545 (2012).
58. S. L. Fernandez-Valverde, R. J. Taft, J. S. Mattick, Dynamic isomiR regulation in *Drosophila* development. *RNA* **16**, 1881–1888 (2010).
59. T. Katoh, Y. Sakaguchi, K. Miyauchi, T. Suzuki, S.-i. Kashiwabara, T. Baba, T. Suzuki, Selective stabilization of mammalian microRNAs by 3′ adenylation mediated by the cytoplasmic poly(A) polymerase GLD-2. *Genes Dev.* **23**, 433–438 (2009).
60. D. C. Barnard, K. Ryan, J. L. Manley, J. D. Richter, Symplekin and xGLD-2 are required for CPEB-mediated cytoplasmic polyadenylation. *Cell* **119**, 641–651 (2004).
61. T. Nakanishi, H. Kubota, N. Ishibashi, S. Kumagai, H. Watanabe, M. Yamashita, S.-i. Kashiwabara, K. Miyado, T. Baba, Possible role of mouse poly(A) polymerase mGLD-2 during oocyte maturation. *Dev. Biol.* **289**, 115–126 (2006).
62. L. Rouhana, L. Wang, N. Buter, J. E. Kwak, C. A. Schiltz, T. Gonzalez, A. E. Kelley, C. F. Landry, M. Wickens, Vertebrate GLD2 poly(A) polymerases in the germline and the brain. *RNA* **11**, 1117–1130 (2005).
63. M. Lee, Y. Choi, K. Kim, H. Jin, J. Lim, T. A. Nguyen, J. Yang, M. Jeong, A. J. Giraldez, H. Yang, D. J. Patel, V. N. Kim, Adenylation of maternally inherited microRNAs by wispy. *Mol. Cell* **56**, 696–707 (2014).
64. T. Hamatani, M. G. Carter, A. A. Sharov, M. S. H. Ko, Dynamics of global gene expression changes during mouse preimplantation development. *Dev. Cell* **6**, 117–131 (2004).
65. C. B. Kimmel, W. W. Ballard, S. R. Kimmel, B. Ullmann, T. F. Schilling, Stages of embryonic development of the zebrafish. *Dev. Dyn.* **203**, 253–310 (1995).
66. Y. Wang, R. Medvid, C. Melton, R. Jaenisch, R. Blelloch, DGCR8 is essential for microRNA biogenesis and silencing of embryonic stem cell self-renewal. *Nat. Genet.* **39**, 380–385 (2007).
67. D. P. Bartel, C.-Z. Chen, Micromanagers of gene expression: The potentially widespread influence of metazoan microRNAs. *Nat. Rev. Genet.* **5**, 396–400 (2004).
68. A. Eulalio, I. Behm-Ansmant, D. Schweizer, E. Izaurralde, P-body formation is a consequence, not the cause, of RNA-mediated gene silencing. *Mol. Cell. Biol.* **27**, 3970–3981 (2007).
69. M. Flemr, J. Ma, R. M. Schultz, P. Svoboda, P-body loss is concomitant with formation of a messenger RNA storage domain in mouse oocytes. *Biol. Reprod.* **82**, 1008–1017 (2010).
70. R. Parker, U. Sheth, P bodies and the control of mRNA translation and degradation. *Mol. Cell* **25**, 635–646 (2007).
71. T.-P. Gu, F. Guo, H. Yang, H.-P. Wu, G.-F. Xu, W. Liu, Z.-G. Xie, L. Shi, X. He, S.-g. Jin, K. Iqbal, Y. G. Shi, Z. Deng, P. E. Szabó, G. P. Pfeifer, J. Li, G.-L. Xu, The role of Tet3 DNA dioxygenase in epigenetic reprogramming by oocytes. *Nature* **477**, 606–610 (2011).
72. Y.-K. Kim, J. Yeo, B. Kim, M. Ha, V. N. Kim, Short structured RNAs with low GC content are selectively lost during extraction from a small number of cells. *Mol. Cell* **46**, 893–895 (2012).
73. F. Tang F. Tang, P. Hajkova, S. C. Barton, D. O'Carroll, C. Lee, K. Lao, M. A. Surani, 220-plex microRNA expression profile of a single cell. *Nat. Protoc.* **1**, 1154–1159 (2006).
74. R. Shi, V. L. Chiang, Facile means for quantifying microRNA expression by real-time PCR. *Biotechniques* **39**, 519–525 (2005).

Acknowledgments: We thank Y. Zhao for the critical reading and correction of the manuscript and C. Shi for technique assistance in qRT-PCR analyses of low-input RNA. **Funding:** This work was supported by the Ministry of Science and Technology of China (2012CB910802 to L.W. and 2014CB943100 to H.S.), the Chinese Academy of Sciences–Shanghai Science Research Center (CAS-SSRC-YJ-2015-01 to L.W.), the National Natural Science Foundation of China (91440107 and 31470781 to L.W.), the Shanghai Municipal Commission for Science and Technology (12JC1409400 to L.W.), and the State Key Laboratory of Molecular Biology. **Author contributions:** Q.Y., H.S., and L.W. conceived and designed the study. J.L. and R.L. performed the computational analysis. Q.Y. constructed the cDNA libraries of small RNAs and performed the qRT-PCR assays. Miao Liu performed the mouse embryo and sperm experiments. Xue Zhang and B.X. contributed to the experimental validation. Mofang Liu, Xuan Zhang, and Y.L. designed the studies in embryos and sperms. B.T. designed the initial protocol for sequencing small RNA. J.L., R.L., Q.Y., B.T., and L.W. wrote the manuscript. **Competing interests:** The authors declare that they have no competing interests. **Data and materials availability:** All data needed to evaluate the conclusions in the paper are present in the paper and/or the Supplementary Materials. The deep sequencing data have been deposited in the Sequence Read Archive of the National Center for Biotechnology Information under accession no. SRP045287. Additional data related to this paper may be requested from the authors.

Submitted 19 October 2015
Accepted 20 May 2016
Published 10 June 2016
10.1126/sciadv.1501482

Citation: Q. Yang, J. Lin, M. Liu, R. Li, B. Tian, X. Zhang, B. Xu, M. Liu, X. Zhang, Y. Li, H. Shi, L. Wu, Highly sensitive sequencing reveals dynamic modifications and activities of small RNAs in mouse oocytes and early embryos. *Sci. Adv.* **2**, e1501482 (2016).